ELSEVIER

Deep-Sea Research II 51 (2004) 927–943

DEEP-SEA RESEARCH
PART II

www.elsevier.com/locate/dsr2

Processes of coastal upwelling and carbon flux in the Cariaco Basin

Frank Muller-Karger[a,*], Ramon Varela[b], Robert Thunell[c], Yrene Astor[b], Haiying Zhang[a], Remy Luerssen[a], Chuanmin Hu[a]

[a]*College of Marine Science, University of South Florida, St. Petersburg, FL 33701, USA*
[b]*Fundacion La Salle de Ciencias Naturales, Estacion de Investigaciones Marinas de Margarita, Apartado 144 Porlamar, Isla de Margarita, Venezuela*
[c]*Department of Geological Sciences, University of South Carolina, Columbia, SC 29208, USA*

Received 18 September 2002; accepted 6 October 2003
Available online 15 September 2004

Abstract

Monthly hydrographic, phytoplankton biomass and primary production, bio-optical observations, and settling particulate organic carbon flux observations were collected at 10.5°N, 64.67°W within the Cariaco Basin, off Venezuela, for a period exceeding seven years starting in November 1995. These data were combined with a time series of Sea-viewing Wide-Field-of-view Sensor (SeaWiFS), advanced very high-resolution radiometer (AVHRR), and European Remote Sensing Satellite/QuikScat data to examine the spatial extent of a cold coastal upwelling plume and a phytoplankton bloom associated with it. The seasonal upwelling cycle was directly linked to the intensity of the Trade Winds, with sea-surface temperature (SST) changes lagging the wind by 1–2 weeks. The seasonal cycle of most properties was punctuated by transient phenomena, some of which caused subsurface ventilation and also high primary production events. Integrated primary production ranged from 650, 574, and 593 g C m^{-2} yr^{-1} in 1996, 1997, and 2001, respectively, to 372, 484, and 448 g C m^{-2} yr^{-1}, respectively, in 1998, 1999, and 2000. The Rutgers vertical generalized production model (VGPM) was modified to reflect an increase in Assimilation Number (PB^{opt}) with SST at the Cariaco time series station, because the original VGPM formulation suggested inhibition of primary production at SST > 21°C. Trap observations showed that between 9 and 10 g C m^{-2} yr^{-1} were delivered to the bottom at the Cariaco time series station, i.e. ~1.33% of surface primary productivity. Annual particulate organic carbon flux to the bottom over the area of the Cariaco Basin (waters > 100 m), estimated using SeaWiFS and AVHRR variable inputs and the updated VGPM, ranged from 6.77×10^{10} to 7.61×10^{10} g C. These are likely underestimates due to lack of bathymetric corrections to flux.

*Corresponding author. Tel.: +1-727-553-3335; fax: +1-727-553-1103.
E-mail address: carib@marine.usf.edu (F. Muller-Karger).

0967-0645/$ - see front matter © 2004 Elsevier Ltd. All rights reserved.
doi:10.1016/j.dsr2.2003.10.010

1. Introduction

Over geological time scales, geochemical imbalances at the Earth's surface are closely tied to carbon sequestration by marine organisms. However, whether this mechanism helps mitigate the increase of anthropogenic greenhouse gases over years to decades represents one of the most pressing questions in oceanography (Longhurst, 1991; de Haas et al., 2002). As we enter the new millennium, only a handful of multi-year time series of in situ observations are available to study the connection between surface primary production and vertical carbon flux in the ocean. Clearly, it is not practical to conduct such detailed in situ observations in more than a few carefully selected locations. Space-based observations therefore offer promise in the effort to quantify global ocean productivity (Falkowski, 2002; Geider et al., 2001; Behrenfeld et al., 2001), but an important additional step is to assess the applicability of satellite data to assessing particulate carbon flux to the bottom of the ocean (e.g., Deuser et al., 1988, 1990). Here we address this question by studying time series observations collected within the Cariaco Basin.

1.1. Geographic setting and significance of the Cariaco Basin

The Cariaco Basin (Fig. 1) is a 1400 m deep depression on the continental shelf off Venezuela. It is openly connected to the surface Atlantic Ocean above a shallow (~100 m) sill. There are two channels breaching this sill, one in the northeast of 135 m depth (La Tortuga) and a narrower one in the northwest of 146 m (Centinela)(Richards, 1975; Lidz et al., 1969). The sill restricts water motion and lateral exchange of material with the adjacent ocean. We may view the Cariaco Basin conceptually as a natural sediment trap within a continental shelf. Because turnover of basin waters is slow (Deuser, 1973), decomposition of the sinking material leads to permanent anoxia below about 275 m.

This scenario has served biogeochemists for over 40 years in the construction of stoichiometric models of organic matter remineralization (Redfield et al., 1963; Richards, 1975; Hastings and Emerson, 1988; Zhang and Millero, 1993; Scranton et al., 2001a; Scranton et al., 2001b), development of residence-time and box models (Scranton et al., 1984; Ward et al., 1987), and in the study of metallic sulfides (Bacon et al., 1980), among many other organic matter remineralization and redox-sensitive process studies. The Cariaco Basin is indeed the largest anoxic basin of truly oceanic character and represents an important complement to the Black Sea for chemical oceanographic studies.

More recently, the scientific community has come to appreciate the Cariaco Basin as an exceptional archive of past climate change (Overpeck et al., 1989; Hughen et al., 1996a, b, 1998, 2000; Haug et al., 1998; Black et al., 1999; Peterson et al., 1991, 2000; Werne et al., 2000). It is increasingly evident that the tropics play an important role in global climate, influencing the hydrologic balance between Atlantic and Pacific Oceans, the heat balance between low and high latitudes, and consequently general ocean circulation (Enfield and Mayer, 1997; Giannini et al., 2000, 2001; Hoerling et al., 2002). Corals provide only a short record of tropical climate, making it difficult to assess how past changes observed in ice cores at high latitudes relate to changes in the tropics. Surficial Cariaco Basin sediments instead contain a clear record of the last 15,000 years and have been used to reconstruct changes in the rate of formation of North Atlantic Deep Water and in the surface circulation of the Atlantic Ocean (Hughen et al., 1998, 2000). The most recent ocean drilling program (ODP) cores collected in the Cariaco Basin extend this record back over 600,000 years, and suggest that the modern deposition patterns are observed during past interglacials, and that glacial periods show increased ventilation and diminished organic carbon accumulation in the sediment (Haug et al., 1998).

The quiescent anoxic bottom conditions in the Cariaco Basin and associated absence of bioturbation allow the accumulation of sediment varves at the bottom of the basin in the present-day oceanographic regime. These varves contain the climate record. Each varve is a couplet consisting of a light and a dark layer. The light laminae are

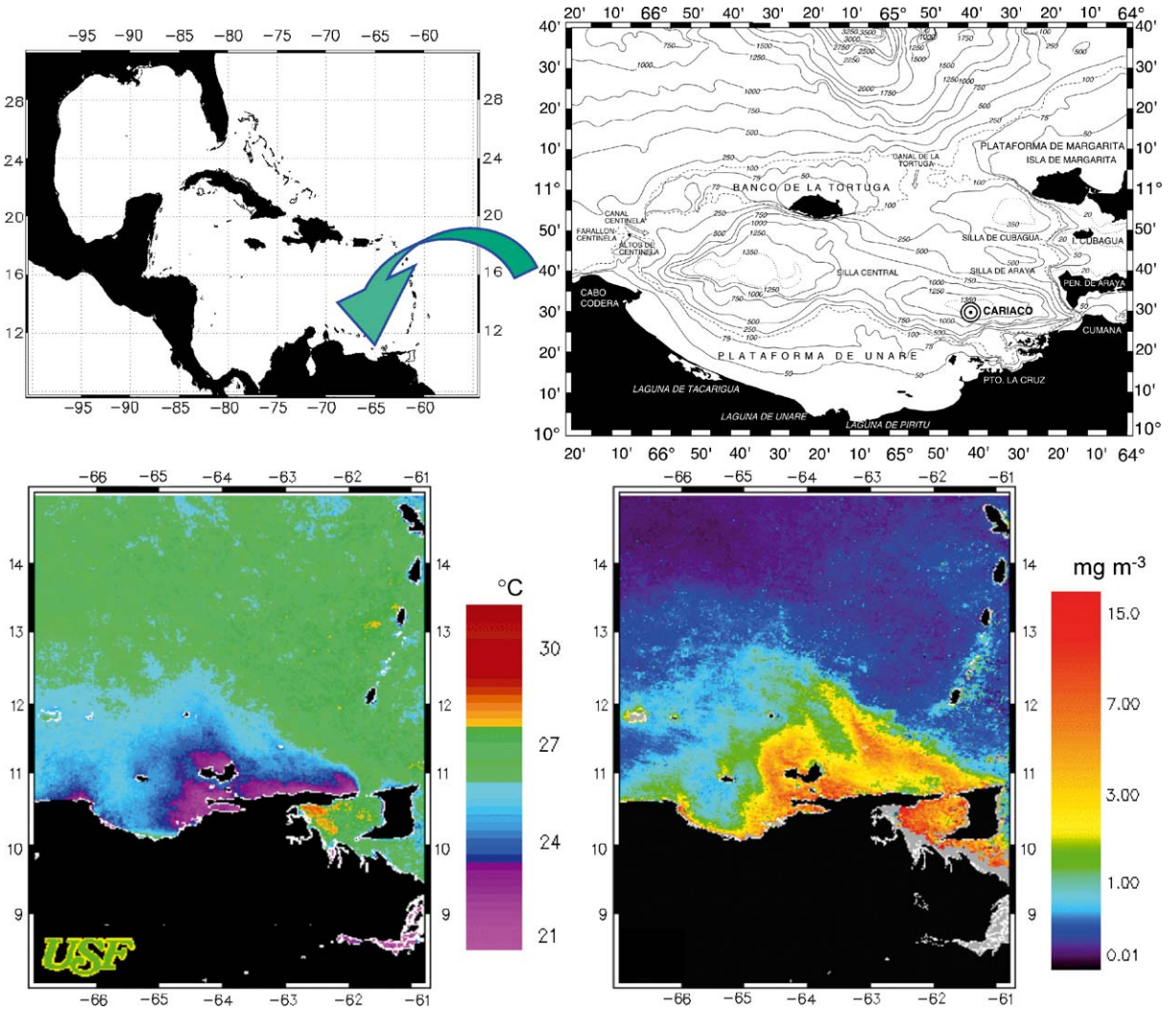

Fig. 1. The Cariaco Basin, location and representative AVHRR and SeaWiFS images. Top left: location of the Cariaco Basin in the Caribbean Sea; top right: Cariaco Basin bathymetry (m) and location of the CARIACO time series station (circle at 10°30′N, 64°40′W); bottom left: monthly AVHRR SST composite (March 2001); bottom right: monthly SeaWiFS Chl-*a* composite (March 2001). Black areas in the images represent land. Gray areas in the SeaWiFS image off the mouth of the Orinoco River represent highly turbid coastal waters.

rich in plankton remains and are thought to be deposited during the upwelling period, or approximately between December and June every year. In contrast, the dark laminae consist of detrital material or terrestrial minerals, presumably delivered to the basin during the rainy season between August and September. Assumptions underlying this simple conceptual model, and specifically assumptions about the origin of materials deposited in the sediment, and about the effect of changes in hydrography, wind, phytoplankton community composition, primary productivity, and terrestrial input, have not been tested.

Indeed, very little is known about carbon fluxes in the tropics, and the Cariaco Basin provides a convenient and unique setting in which to study the connection between near-surface ocean dynamics, variability in primary production, and the

settling of particulate organic carbon to depth within a tropical environment.

2. Methods

We base this study on the CArbon Retention In A Colored Ocean (CARIACO) time series, initiated in November 1995 (Muller-Karger et al., 2000, 2001; Astor et al., 2003; Thunell et al., 1999, 2000; Scranton et al., 2001a, 2001b; Taylor et al., 2001). The time series station is located at 10°30′N, 64°40′W (Fig. 1), where we measured hydrographic variables, primary productivity, and sediment fluxes at multiple depths. Here we focus on the period June 1996 to December 2002, when in situ bio-optical data also were collected. Settling organic particulate carbon flux was measured with sediment traps positioned at approximately 275, 455, 930, and 1225 m, as described by Thunell et al. (2000), within the quiescent flow regime below sill depth. Methods for the CARIACO time series were reviewed by Muller-Karger et al. (2001). Bio-optical data were processed as per Mueller and Austin (1992, 1995) and Fargion and Mueller (2000). The CARIACO data are available to the public via the URL: http://imars.usf.edu/cariaco. Data also are available through the National Ocean Data Center (NODC). Bio-optical data are available via SeaBASS (Fargion, 1999).

We complemented the study with satellite data from the Sea-viewing Wide-Field-of-view Sensor (SeaWiFS), the advanced very high-resolution radiometer (AVHRR), and with scatterometer data collected between 1998 and 2002. These are briefly described below.

Since there are no direct wind observations within the Cariaco Basin, wind estimates were obtained using the active microwave instrument (AMI) scatterometer on the European Remote Sensing Satellites 1 and 2 (ERS-1 and ERS-2) for winds between 1995 and 1999 (Pouliquen et al., 1996) and NASA's QuikScat sensor for winds after 1999 (NASA's Jet Propulsion Laboratory). The anemometer data collected at the Margarita Island airport are seriously flawed, as described in Astor et al. (2003). Astor et al. (2003) found that changes in hydrography lag changes in the scatterometer wind by 1–2 weeks. This corrected the spurious results on the phasing between wind and upwelling found based on the anemometer data and published earlier by Muller-Karger et al. (2001).

Sea-surface temperature (SST) was estimated from imagery collected by the AVHRR sensors on the NOAA 11, 12, and 14 satellites. The satellite SSTs were derived using the split-window techniques (Walton, 1988; Strong and McClain, 1984; McClain et al., 1983). While non-linear algorithms developed for AVHRR data could be used, there is no conclusive evidence that these algorithms are any better than the MCSST algorithms. The process of masking clouds in deriving SST from AVHRR data was imperfect, and the SST products showed frequent low temperature patches because of cloud contamination. To remove unreasonably low AVHRR SST observations, individual pixels in scenes that departed by more than a standard deviation from a 10-day running mean were eliminated. Using a linear interpolation, we then reconstructed the series to match the dates of the in situ or the SeaWiFS observations. The nominal accuracy of AVHRR SST retrievals is approximately ± 0.5 K (also see Brown et al., 1985; Minnett, 1991).

The SeaWiFS data used conformed to version 4 products (summer 2002 processing by NASA). This included spatial filtering to reduce digitization noise (e.g., Hu et al., 2001), as well as appropriate calibration corrections of the blue bands, sophisticated atmospheric correction (Arnone et al., 1998; Gordon and Wang, 1994; Ding and Gordon, 1995) and a bio-optical algorithm to estimate chlorophyll-*a* (Chl-*a*) concentration (O'Reilly et al., 2000). The data were systematically calibrated by NASA to meet mission specifications (McClain et al., 1998; Barnes et al., 1999), which called for less than $\pm 35\%$ uncertainties in the Chl-*a* concentration retrievals.

Each of the SeaWiFS and the AVHRR image products was mapped to the same cylindrical equidistant projection, so that all products of the same type were spatially congruent. They were then binned to create eight-day and monthly composites. The spatial resolution of the SST images was $1.5 \times 2.0\,\mathrm{km}^2$ per pixel, and those representing Chl and primary productivity were $9 \times 9\,\mathrm{km}^2$ per pixel. Sampling at the CARIACO

station was accomplished by extracting a single SeaWiFS Chl pixel (i.e., $9 \times 9\,km^2$). Therefore, spatial variability of Chl estimates within the sample pixel was not examined. A 5×5 pixel box was used for extracting SST from the AVHRR imagery.

The temporal variation in the spatial dimensions of the upwelling plume was estimated with AVHRR-derived SST and SeaWiFS-derived Chl-*a* products. This was accomplished by defining a mask that encompassed Cariaco Basin waters deeper than 100 m. Thus, the mask included waters seaward of the southern edge of the Basin, which receives the discharge of a few small rivers, and extended up to the northern sill. The area where SST was $<26\,^{\circ}C$ was used to define the plume in AVHRR images, and a threshold of 0.4 mg Chl-$a\,m^{-3}$ traced the surface area of the plume in SeaWiFS images. Area was estimated by multiplying the area of one pixel by the number of pixels counted within the patch defined as the upwelling plume in each image. The area of each pixel within each image was a constant, as defined above.

To fulfill our objective to use the CARIACO time series as a calibration point for regional satellite-derived primary productivity assessments, we tested the empirical vertical generalized production model (VGPM; Behrenfeld and Falkowski, 1997a, b; Falkowski et al., 1998). We tested the VGPM using only in situ data (optics and photosynthetically active radiation (PAR) data, Chl-*a*, and temperature) to model primary productivity. We found a need to reformulate the PB^{opt} algorithm included in the model, and we did this using local Assimilation Number (PB^{opt}) and SST data collected between 1996 and 2001. The VGPM also was run using only remotely sensed parameters (PAR, SST, and Chl-*a*) and our modified PB^{opt} algorithm. The validity of the reformulated VGPM was tested with independent data collected in 2002.

3. Results and discussion

3.1. Winds and hydrography

Fig. 1 depicts typical conditions observed in satellite data during March, when a large area of the southeastern Caribbean experiences SST below 25°C. Some of the lowest SST are observed along the southeastern margin of the Cariaco Basin. At the CARIACO station, the lowest SST (21.5–24 °C) appeared between February and March (Fig. 2). These low temperatures were associated with a seasonally varying upwelling plume that reached well over $10{,}000\,km^2$ when fully extended. High SST ($>28\,^{\circ}C$) typically occurred between August and October. A secondary and very short-lived upwelling event was observed every year around July, but this led only to minor, if any, cooling at the surface. A cross-correlation analysis between weekly mean satellite-derived SST and weekly mean scalar wind intensity showed a peak in correlation at a positive lag of 1–2 weeks (see Astor et al., 2003), which provided an estimate for the time scale of response of the upwelling to changes in the wind.

Astor et al. (2003) described the variability in wind at the CARIACO station. Briefly, the wind was predominantly westward and followed a marked seasonal cycle in intensity. Scalar and westward wind speeds weaker than $6\,m\,s^{-1}$ occurred between approximately July and November (Fig. 2). Seasonal maxima $>6\,m\,s^{-1}$ occurred between November and May. Overall, 1999 showed the weakest winds relative to all other years. In 1999, we observed a near-reversal in February and a month-long wind reversal in November. In 1996 and 2002, westward winds were strong in August and September. July showed the least interannual variability during the series. The meridional (north–south) component of the wind (range -5 to $1\,m\,s^{-1}$) was typically much weaker than the zonal wind and was frequently nil. This component intensified slightly toward the south between July (minima in intensity) and approximately December (southward maxima).

Salinity profiles also allowed us to examine upwelling and track the influence of various water masses at the CARIACO station. The core of the salinity maximum (>36.8; Subtropical Underwater) was located near 130 m in July, but the upper boundary of this layer moved upward and reached depths shallower than 50 m between January and June. During upwelling periods,

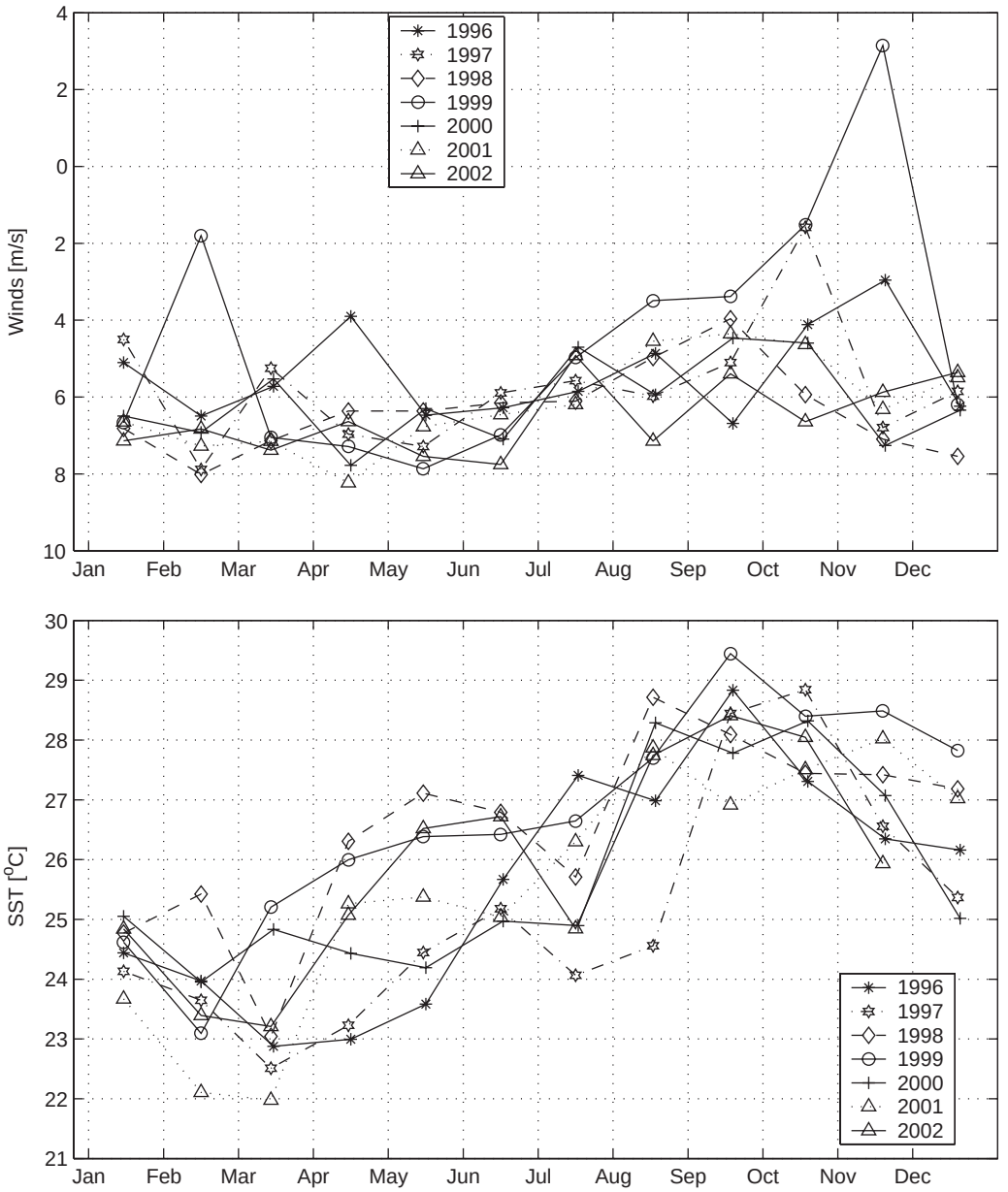

Fig. 2. Top: monthly mean westward component of the Trade Wind (u, $m\,s^{-1}$) estimated with the ERS-1/2 and QuikScat satellite scatterometers (1996–2002). Bottom: in situ SST (°C) obtained during the CARIACO monthly cruises (1996–2002).

silicate concentrations of only 0–0.5 μM were observed at the surface. A relatively fresh surface layer (~36.3) appeared during August–October. Low surface salinities between August and October coincided with warmer surface temperatures. More significantly, the low surface salinities were associated with an increase in the surface silicate concentration, reaching values of 1–3 μM coincident with salinity minima. These indicated an increase in the influence of terrestrial runoff on the basin. In 1999, the period of low surface salinity extended from approximately July to December,

with extremely low salinities and high silicate between October and December. This event was associated with torrential and catastrophic rains along the Venezuelan coastline.

3.2. Phytoplankton biomass (Chl-a) and productivity

Fig. 1 shows the spatial extent covered by a typical phytoplankton bloom in the southern Caribbean during upwelling in March. High concentrations of Chl-*a* extended seaward off the continent in a northwestward direction and engulfed the island of Margarita. High concentrations of Chl-*a* also were apparent within the Gulf of Paria and north of Trinidad (in the eastern half of the image), but these were not associated with cooler SSTs. Indeed, the values in the Gulf of Paria and north of Trinidad are artificially higher because of colored dissolved organic matter (CDOM) in the Amazon and Orinoco River plumes (see Hu et al., 2004; Muller-Karger et al., 1989).

The time series of monthly observations revealed strong seasonal and interannual variation in both the Chl-*a* concentration and the depth-integrated (100 m) primary productivity at the CARIACO station (Fig. 3). Integrated Chl-*a* (100 m) showed a strong inverse correlation with SST (cross-correlation = −0.77 at zero lag; $n = 83$; not shown). These cold waters have higher nutrient concentrations than the surface waters they replace, and this stimulates the observed phytoplankton growth.

It was not possible to derive a rigorous cross-reference data set between SeaWiFS and in situ Chl-*a* observations (or productivity estimates) because only six matched pairs were obtained, even using eight-day windows for the SeaWiFS composites. To assess the SeaWiFS Chl-*a* we constructed an artificial set of matched-up data pairs by interpolating the eight-day SeaWiFS product to the date of the monthly CARIACO observation. The artificial match-ups produced an $r^2 = 0.71$ ($N = 51$; slope $m = 0.51$ and intercept $b = 0.61$). Fig. 3 also shows that, on average, SeaWiFS overestimated in situ Chl, particularly when low in situ values were observed but occasionally also at intermediate and higher in situ values.

The reason for the overestimate of Chl-*a* was not clear. Small rivers draining into the Cariaco Basin affect surface salinity at the CARIACO station in September and October, i.e. during the rainy season. These rivers may contain sufficient CDOM to affect concentrations derived from ocean-color data. Surface CDOM absorption (a_g (440 nm)) data collected at the CARIACO station in 2002–2003 showed low values ranging from 0 in June and July in low Chl water to 0.07 m^{-1} in August 2002 under riverine influence. Fresh water influx into this area during the upwelling season is expected to be minimal, however. The large river plumes from the Orinoco and Amazon Rivers also have minimal influence within the Cariaco Basin at all times (Muller-Karger et al., 1989; Muller-Karger and Varela, 1990). During the upwelling season, it is possible that the upwelling source water is colored by high background CDOM, as suggested for other upwelling zones (Siegel et al., 2002; Coble et al., 1998).

During upwelling months, a_g (440 nm) values were variable, ranging between 0.02 and 0.05 m^{-1} but reaching 0.07 m^{-1} in March of both 2002 and 2003. Values of 0.09 m^{-1} were seen in January 2003. Due to insufficient data, it was not possible to determine whether the higher CDOM absorption occurred in the upwelling source water prior to entering the Cariaco Basin, or whether it was autochthonous.

Depth-integrated Chl and primary productivity showed a strong relationship. Indeed, by eliminating less than 3% of points that could be considered outliers during periods of high Chl or productivity, over 70% of the variation in primary production could be accounted for by changes in integrated Chl. There was typically one large production event per year, which lasted 1–3 months. Average integrated annual production (six years) was 525 g C m^{-2}. The most productive years (>570 g C m^{-2} yr) were 1996, 1997, and 2001, and 1998 was the least productive (<372 g C m^{-2} yr^{-1}). Upwelling in early 1998 was weak, which may have been related to the 1997–1998 El Niño-Southern Oscillation (ENSO). Changes in meteorological conditions in the Caribbean that seem coincident with ENSO have been observed previously (Enfield and Mayer, 1997; Giannini et al.,

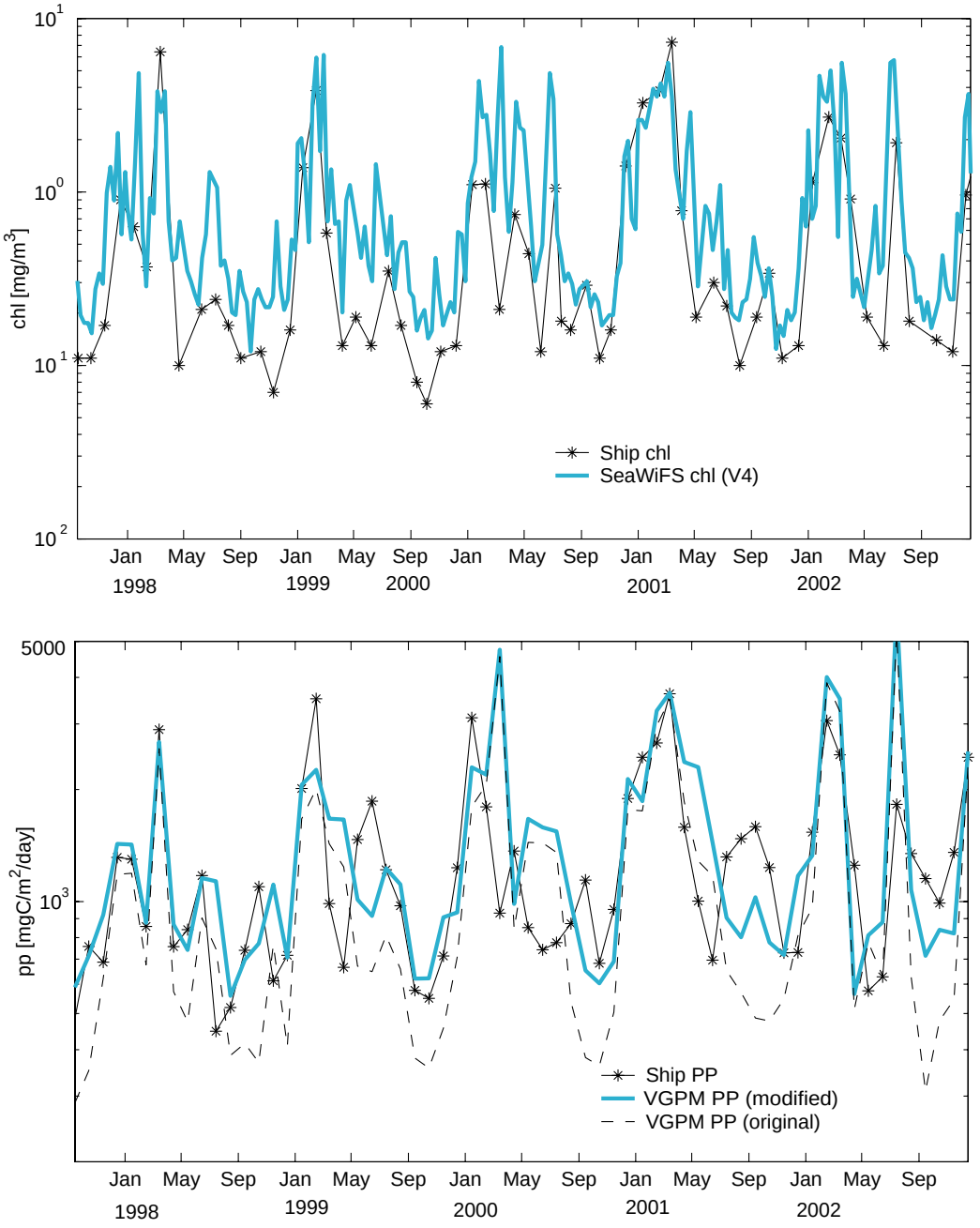

Fig. 3. Top: surface in situ (solid line, asterisks) and SeaWiFS-derived (version 4) Chl-*a* (thick gray line) at the CARIACO station. The SeaWiFS-derived Chl data were obtained by sampling a single $9 \times 9\,km^2$ pixel centered on the CARIACO station. Bottom: in situ (solid line, asterisks) and modeled primary productivity estimates of depth-integrated (100 m) daily production, derived with the original (broken line) and the modified (thick gray line) VGPM based on satellite data input parameters. Log scaling used to emphasize differences between the series.

2000, 2001; Hoerling et al., 2002), but the mechanisms that would lead to such connections are not yet clear.

We tested the VGPM (Behrenfeld and Falkowski, 1997a) using in situ (SST, PAR, and Chl-*a*) and satellite-derived (SST, PAR, and Chl-*a*) data separately. The VGPM results obtained with these independent data showed similar temporal variability as the in situ primary production observations. Fig. 3 shows the results obtained using satellite input parameters as well as the actual in situ productivity observations. The VGPM results using in situ input parameters (not shown in Fig. 3) were lower than those obtained using satellite-derived input parameters, which was expected because of the SeaWiFS Chl overestimate. Particularly during periods of productivity minima, both simulations underestimated the in situ primary productivity. Values during productivity peaks matched the general magnitude of the in situ measurements.

We studied the VGPM and input parameters to determine the possible source of the mismatch during periods of low productivity. We found that PAR effectively played a minor role in the VGPM (also see Behrenfeld and Falkowski, 1997b). Further, modeled euphotic depths compared well with euphotic depths estimated from in situ data. Clearly, the SeaWiFS Chl-*a* did not explain why the VGPM underestimated in situ production either, since the satellite data overestimated in situ Chl, particularly during low-Chl periods (Fig. 3), and VGPM productivity is a direct function of surface Chl concentration.

We found one likely explanation for the mismatch in the PB^{opt} photoadaptive parameter (Behrenfeld and Falkowski, 1997a). Muller-Karger et al. (2001) noticed that the PB^{opt} parameter obtained during the CARIACO series was typically higher than that predicted by Behrenfeld and Falkowski (1997a). PB^{opt} at CARIACO, which generally occurred around 7 m, followed a seasonal cycle in direct proportion to SST, and did not decline at SST $>21\,^{\circ}C$ as formulated by Behrenfeld and Falkowski (1997a).

Clearly, there has been substantial latitude in the definition of the PB^{opt} photoadaptive parameter or equivalent (Behrenfeld and Falkowski, 1997b), with most formulations showing drastic inhibition in photosynthesis at temperatures >15–$21\,^{\circ}C$. Behrenfeld et al. (2002) have recently suggested that temperature has a negligible influence on PB^{max} and PB^{opt} above $5\,^{\circ}C$. Nevertheless, the CARIACO data behave differently. Our data do not suggest inhibition of photosynthesis even at temperatures as high as $29\,^{\circ}C$, and indeed CARIACO values behave similar to the maximum specific growth rates of Eppley (1972) after conversion to carbon fixation as described in Behrenfeld and Falkowski (1997b) and Antoine et al. (1996).

SSTs in the Cariaco Basin, as in most of the tropics, are typically above $21\,^{\circ}C$. Therefore, we computed a new seventh-order polynomial to model PB^{opt} based on SST at CARIACO, and merged this with the model of Behrenfeld and Falkowski (1997a) for temperatures $<21\,^{\circ}C$ (we arbitrarily weighted each of the points shown in Fig. 7 of Behrenfeld and Falkowski (1997a), by a factor of 5 and binned these points with the CARIACO data). This new relationship spans a broader SST range, reaching $29.5\,^{\circ}C$. Waters outside the Cariaco Basin may reach temperatures $>30^{\circ}C$, but we had no data to assess the applicability of the polynomial in these conditions. The new polynomial is

$$PB^{opt} = A*SST^7 + B*SST^6 + C*SST^5 + D*SST^4 + E*SST^3 + F*SST^2 + G*SST + H,$$

where $A=-0.00000019075$, $B=0.00001847528$, $C=-0.00068620340$, $D=0.01212491779$, $E=-0.10165597657$, $F=0.33672550197$, $G=0.10336875858$, and $H=1.00022697060$. Significant digits are retained. SST range is between 21 and $29.5\,^{\circ}C$. Outside this range we would revert to the original Behrenfeld and Falkowski (1997a) model.

Fig. 3 shows the improvement in the modeled primary production based on satellite input parameters relative to the original algorithm. Similar results were obtained with the modified VGPM based on the ship input parameters.

Since the VGPM results depend on an accurate input biomass value, the effects of a biased

SeaWiFS Chl-*a* estimate are confounded here with the new relationship between SST and PB^{opt}. The relationship proposed here works well with the SeaWiFS version 4 products, released in 2002.

3.3. Upwelling plume surface area

The upwelling phenomenon caused depressed surface temperatures and elevated Chl concentrations. The patch of cooler temperatures was clear in AVHRR imagery. In an attempt to define whether there was a direct relationship between the area over which the cold upwelled waters spread and the size of the phytoplankton bloom, we estimated the surface area covered by the upwelling plume over the Cariaco Basin based on AVHRR and SeaWiFS images. A threshold of 26 °C for SST and of 0.4 mg Chl-a m^{-3} traced similar surface areas in space and time (Fig. 4). Effectively, within the region bounded by the 100 m isobath inside the Cariaco Basin, the seasonal plume covered a surface area that ranged between 0 and 1×10^3 km^2 from August to October, and which then typically extended over an area greater than 11×10^3 km^2 in March. Lower SST thresholds showed the same seasonal pattern, but yielded a much smaller surface area relative to the Chl plume defined by the 0.4 mg Chl-a m^{-3} isopleth.

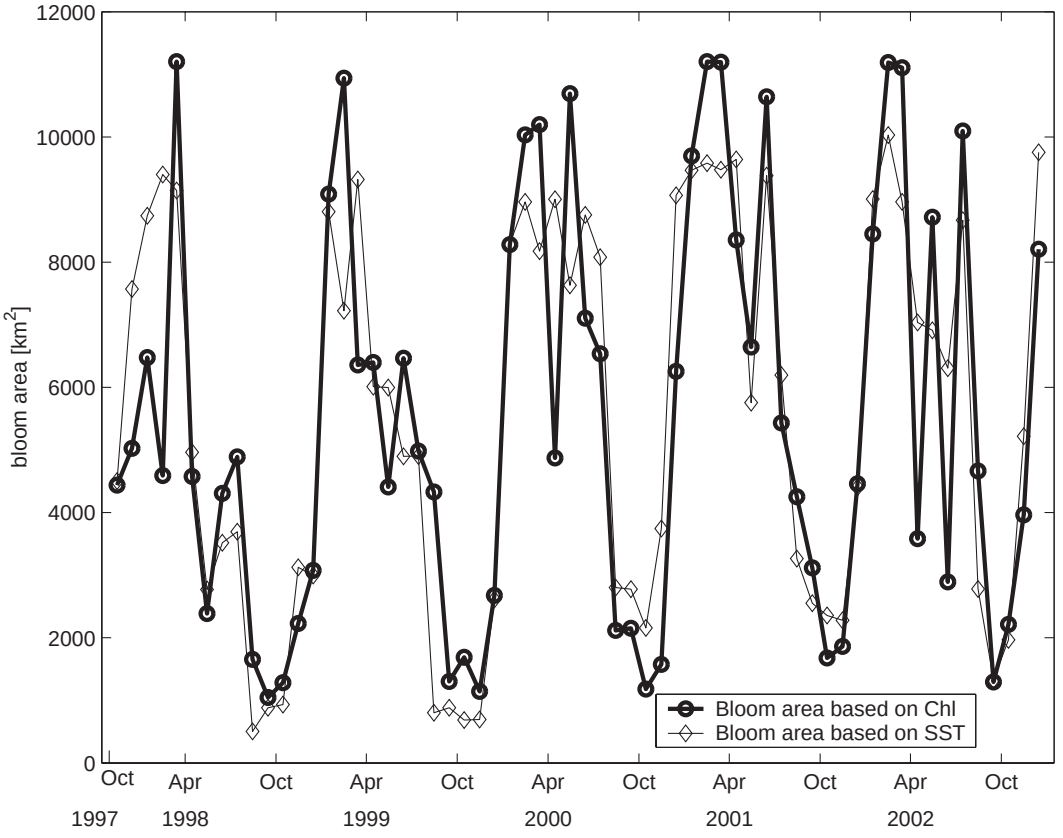

Fig. 4. Surface area (km^2) covered by the upwelling plume at the ocean's surface in waters contained by the 100 m isobath within the Cariaco Basin, determined based on AVHRR and SeaWiFS satellite data. The size of the cold upwelling plume was estimated by counting pixels with SST lower than 26 °C in AVHRR SST images. The size of the phytoplankton bloom was obtained by tracing values of Chl-*a* higher than 0.4 mg Chl-a m^{-3}.

3.4. Sediment trapping results: vertical particulate organic carbon flux

The first six months of sediment trap samples were retrieved successfully in May 1996. Unfortunately, the four traps clogged immediately after redeployment of the mooring, resulting in a data gap in the sediment flux series from May to November 1996. We attributed this to unusually high particle fluxes caused by the large and very anomalous plankton bloom of May 1996 (see Muller-Karger et al., 2001). We experienced another gap from May to November 2001 when the mooring releases did not respond.

The particulate organic carbon flux showed both seasonal and interannual variation in the timing and magnitude of the annual particulate organic carbon flux maxima (Fig. 5). Peaks in the shallowest trap (275 m) typically ranged 100–180 mg C $m^{-2} d^{-1}$, occurred in the February–May timeframe, and lasted for about one month (traps were programmed to collect individual samples over two-week intervals each). The longest peak occurred in 1997 and lasted three months (March–May). Substantial variability was observed in late 1999 and early 2000, when torrential rains afflicted the northern Venezuela coast.

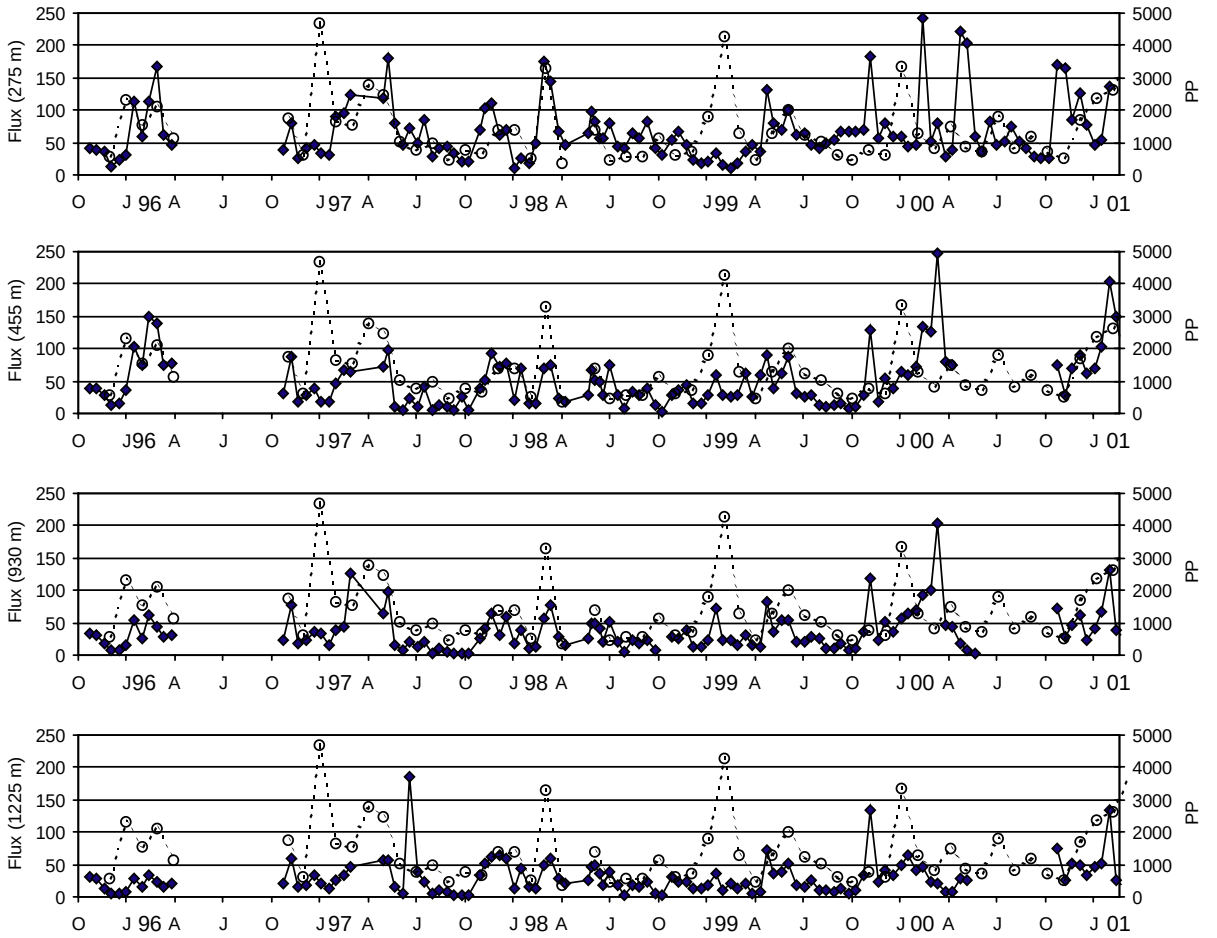

Fig. 5. Time series of CARIACO particulate organic carbon flux (solid line, filled diamonds) captured with sediment traps (mg C $m^{-2} d^{-1}$) at (top to bottom) 275, 455, 930, and 1225 m. Surface primary productivity (broken line, circles) integrated to 100 m (mg C $m^{-2} d^{-1}$) is overlaid on each panel.

Flux generally decreased with depth, and except for a few anomalies the temporal variability observed in the shallowest trap (275 m) was preserved in the three deeper traps as well (Muller-Karger et al., 2001; Thunell et al., 2000). A cross-correlation analysis of the flux captured at traps 1 and 2 (275 and 455 m) showed a correlation of 0.9 at zero lag (i.e., within two-week periods). The largest organic carbon flux prior to the rains of 1999–2000, recorded in the 1225 m trap in early July 1997, was associated with a turbidite generated by a nearby earthquake (Thunell et al., 1999). The highest planktonic flux (estimated at 180 mg $C\,m^{-2}\,d^{-1}$) was observed in the shallowest trap in May 1997.

Earlier results based on only the first two years of paired primary productivity and particulate organic carbon flux observations suggested that there was a good relationship between these variables except for anomalies like the one related to the earthquake (Thunell et al., 2000; Muller-Karger et al., 2001). Preservation of organic matter within the anoxic environment of the Cariaco Basin did not seem to be either enhanced or diminished relative to that seen in other continental margins (Thunell et al., 2000). The longer series available for this study verified that variability in the particulate organic carbon flux at the shallowest trap (275 m) tracked primary productivity, except during extreme surface production events (productivity >3000 mg $C\,m^{-2}\,d^{-1}$). Indeed, such extreme production events were most frequently associated with minima in the flux to the surface trap (values as low as 10 mg $C\,m^{-2}\,d^{-1}$). These flux minima occurred between September and December, i.e. toward the beginning of the annual upwelling season, and appeared to be coincident with episodes of extreme Trade Wind strength.

3.5. Regional particulate organic carbon flux

The material captured by the deepest trap (1225 m) would be the most directly related to the organic particulate carbon deposited at the bottom of the Cariaco Basin. Substituting the turbidite sample of July 1997 by a value approximated by that observed in previous and following months, the three years of full observations (1997, 1998, and 1999) show an annual integrated particulate organic flux of 9.98, 9.33, and 9.56 g $C\,m^{-2}$ to the bottom sediment of the Cariaco Basin every year. The lower flux estimated for 1998 reflected the lower primary productivity observed that year at the surface. These values agreed well with the 7–8 g $C\,m^{-2}\,yr^{-1}$ seen at 2300 m at other continental margin locations (cf. Walsh, 1991; Pilskaln et al., 1996; Etcheber et al., 1996; Thunell, 1998).

A first-order estimate of the flux of particulate organic carbon to the bottom of the Cariaco Basin during blooming periods may be derived assuming that the POC flux to the bottom at the CARIACO station is representative for the entire region. By assuming that the entire Cariaco Basin deeper than 100 m ($\sim 1.12 \times 10^4\,km^2$) experiences similar flux as that observed at CARIACO, we estimate a total annual flux of $\sim 1 \times 10^{11}$ g C to the bottom in both 1998 and 1999.

We may instead assume that such flux occurs only underneath the highly productive upwelling plume, which varies in both spatial extent and in time (Fig. 4). We therefore interpolated the surface area estimates derived from the SeaWiFS data to the dates of trap sample collections, multiplied this with the flux in the deepest trap (1225 m) over the collection interval, and integrated these values over annual periods for 1998 and 1999, i.e. the initial years for which we had concurrent SeaWiFS and trap data. The results suggested that some 5.53×10^{10} g C were collected within the Cariaco Basin under the upwelling plume in 1998, compared to 5.00×10^{10} g C in 1999. This estimate is about half that obtained above, because the plume has a strong seasonal variation and on occasion is much smaller than the Cariaco Basin.

These numbers are not accurate because both our area estimates include regions where bottom depth is shallower than 1225 m and flux at shallower depths is higher than that observed at 1225 m at the CARIACO station. Also, the flux observed at the CARIACO station, located in the eastern portion of the Cariaco Basin, is probably higher than that in the western half of the Basin, where primary productivity is likely lower.

The POC flux collected by traps at 455 and 930 m showed high correlation ($r\sim0.6$) with the SeaWiFS–VGPM results integrated over successive trap sampling intervals. We found very low correlation between the POC flux to the 275 m trap and the SeaWiFS–VGPM results, possibly because of circulation processes or disturbances of the trap material by vertically migrating grazers. The POC flux to the 1225 trap was on occasion strongly affected by material that did not settle from the surface, leading to an intermediate correlation of ($r\sim0.4$). Excluding anomalous POC flux values due to the possible turbidite of July 1997, as we did above, and during extreme primary production events (>3 g C m^{-2} d^{-1}), the deep trap (1225 m) captured on average 1.33% of the surface primary productivity (Flux $\approx 0.0133PP + 153.7$; $r\sim0.44$).

With this information, and multiplexing (or "fusing") the data streams from SeaWiFS and the AVHRR using the VGPM, we attempted to derive a regional estimate of particulate organic carbon delivered to the bottom of the Cariaco Basin. The eight-day composite SeaWiFS-derived PAR plus Chl-*a* and AVHRR SST images, pooled for the period September 1997 to February 2002, were mapped to congruent 9×9 km^2 resolution grids. For waters deeper than 100 m within the Cariaco Basin, this represented a total of 138 grid pixels. We derived daily VGPM at each pixel using our updated PB^{opt}, applied the above relationship to obtain flux (i.e., Flux $= 0.0133PP + 153.7$), and integrated over all pixels and time to obtain the total carbon (g C) per year produced within the Cariaco Basin.

The flux estimates for each year were 1998: 6.77×10^{10} g C; 1999: 7.26×10^{10} g C; 2000: 7.38×10^{10} g C; and 2001: 7.61×10^{10} g C. The numbers were not scaled to account for the exponential decrease in flux with depth and varying bathymetry, but this was not within the scope of the study presented here. In this regard, these values represent an underestimate of the total flux to the bottom of the basin.

It is premature to proceed with more complex models and parameterizations at this stage because there are several inconsistencies between the CARIACO data and the various SeaWiFS algorithms that we need to resolve. These include but are not limited to the mismatch between SeaWiFS and CARIACO Chl-*a* concentrations and the poor characterization of the relationship between primary productivity and POC flux. The procedure outlined here is only a first step in using satellite data to assess POC flux to the bottom. We are focusing observations and analysis efforts on addressing these unresolved issues.

4. Conclusions

The present study helps advance our understanding of how satellites may be combined with in situ observations to assess the fate of carbon in the ocean. Time series like CARIACO are critical to make progress in this scientific endeavor. Some of the major conclusions that may be drawn from this research are as follows:

- The seasonal upwelling cycle was directly linked to the intensity of the Trade Winds, with SST changes lagging the wind by 1–2 weeks.
- The seasonal cycle of most properties was punctuated by transient phenomena, some of which caused subsurface ventilation and also high primary production events.
- Integrated primary production at the CARIACO station is high, with values typically exceeding 550 g C m^{-2} yr^{-1}. Occasional lower production years (<400 g C m^{-2} yr^{-1}) may be associated with ENSO events.
- There are still issues with the accuracy of the SeaWiFS Chl-*a* concentration product, even after reprocessing version 4. Typically, SeaWiFS Chl-*a* tended to overestimate in situ observations at the CARIACO station, particularly during periods of low Chl. We speculate that this may be the result of local high elevations of CDOM associated with river discharge. The question of whether upwelling waters contain CDOM generated in remote locations remains unresolved.
- The Rutgers VGPM underestimated primary production at high tropical SSTs (>21 °C), and thus required a new local relationship between Assimilation Number (PB^{opt}) and SST. Our observations were consistent with those of Gong

et al. (2000) for the subtropical East China Sea. The significance of this observation is that previous estimates of global primary productivity using satellites likely underestimate the contribution of the tropics. Much productivity may occur at high temperature and low Chl concentrations over large areas of the tropical and subtropical oceans. Clearly, an inaccurate parameterization of the photoadaptive parameter(s) in such bio-optical productivity models would lead to large errors in global production estimates.

- Regional variability in phytoplankton biomass and primary productivity do not necessarily track global patterns in response to ENSO events; for example Behrenfeld et al. (2001) reported that both global ocean Chl and primary productivity increased between 1997 and 1998 over an ENSO event. Both these quantities decreased at the CARIACO station and in the southeastern Caribbean Sea.
- Trap observations showed that between 9 and 10 g C m^{-2} yr^{-1} were delivered to the bottom at the CARIACO station, i.e. ~1.33% of surface primary productivity. Annual particulate organic carbon flux to the bottom over the area of the Cariaco Basin (waters > 100 m), estimated using SeaWiFS and AVHRR variable inputs and the updated VGPM, ranged from 6.77×10^{10} to 7.61×10^{10} g C (likely underestimates due to lack of bathymetric corrections to flux).

Acknowledgements

This work was supported by the National Science Foundation (NSF Grants OCE-9216626, OCE-9729284, OCE-9401537, OCE-9729697, OCE-9415790, OCE-0118566, and OCE-9711318), the National Aeronautics and Space Administration (NASA Grants NAG5-6448, NAS5-97128, and NAG5-10738), and the Consejo Nacional de Investigaciones Cientificas y Tecnologicas (CONICIT, Venezuela, Grant 96280221). We are indebted to the personnel of the Fundacion La Salle de Ciencias Naturales, Estacion de Investigaciones Marinas Isla Margarita (FLASA/EDIMAR) for their enthusiasm and professional support. In particular, we thank Dr. Pablo Mandazen (*Hermano Gines*, Director, FLASA) for his confidence in our activities, and the crew of the R./V. *Hermano Gines* (FLASA) for their able support at sea. Jonnathan Garcia, Javier Gutierrez, Anadiuska Rondon (all at FLASA/EDIMAR), and John Akl and Ana Lucia Odriozola (at USF) provided essential field and laboratory support. Luis Troccoli, Wilfredo Patiño, Luis Sanchez, and William Senior, from the Universidad de Oriente, Cumana, Venezuela, provided nutrient data. The Biotechnology Laboratory of Empresas Polar in Caracas, Venezuela, has kindly allowed access to their scintillation counter for our primary productivity assessments.

References

Antoine, D., André, J.M., Morel, A., 1996. Oceanic primary production 2. Estimation at global scale from satellite (coastal zone color scanner) chlorophyll. Global Biogeochemical Cycles 10, 57–69.

Arnone, R.A., Martinolich, P., Gould Jr., R.W. Stumpf, R., Ladner, S., 1998. Coastal optical properties using SeaWiFS. SPIE Proceedings, Ocean Optics XIV, Kailua Kona, Hawaii, USA, November 10–13, 1998.

Astor, Y., Muller-Karger, F.E., Scranton, M., 2003. Seasonal and interannual variation in the hydrography of the Cariaco Basin: implications for basin ventilation. Continental Shelf Research 23 (1), 125–144.

Bacon, M.P., Brewer, P.G., Spencer, D.W., Murray, J.W., Goddard, J., 1980. Lead-210, polonium-2210, manganese and iron in the Cariaco Trench. Deep-Sea Research 27, 119–135.

Barnes, R.A., Eplee Jr., R.E., Patt, F.S., McClain, C.R., 1999. Changes in the radiometric sensitivity of SeaWiFS determined from lunar and solar-based measurements. Applied Optics 38, 4649–4664.

Behrenfeld, M.J., Falkowski, P.G., 1997a. Photosynthetic rates derived from satellite-based chlorophyll concentration. Limnology and Oceanography 42 (1), 1–20.

Behrenfeld, M.J., Falkowski, P.G., 1997b. A consumer's guide to phytoplankton primary productivity models. Limnology and Oceanography 42 (7), 1479–1491.

Behrenfeld, M.J., Randerson, J.T., McClain, C.R., Feldman, G.C., Los, S.O., Tucker, C.J., Falkowski, P.J., Field, C.B., Frouin, R., Esaias, W.E., Kolber, D.D., PollackN., H., 2001. Biospheric primary production during an ENSO transition. Science 291, 2594.

Behrenfeld, M.J., Marañón, E., Siegel, D.A., Hooker, S.B., 2002. Photoacclimation and nutrient-based model of light-saturated photosynthesis for quantifying oceanic

primary production. Marine Ecology Progress Series 228, 103–117.

Black, D.E., Peterson, L.C., Overpeck, J.T., Kaplan, A., Evans, M.N., Kashgarian, M., 1999. Eight centuries of North Atlantic Ocean atmosphere variability. Science 286, 1709–1713.

Brown, O.B., Brown, J.W., Evans, R.H., 1985. Calibration of advanced very high resolution radiometer infrared observations. Journal of Geophysical Research 90, 11667–11678.

Coble, P.G., Del Castillo, C.E., Avril, B., 1998. Distribution and optical properties of CDOM in the Arabian Sea during the 1995 Southwest Monsoon. Deep-Sea Research II 45, 2195–2223.

de Haas, H., van Weering, T.C.E., de Stigter, H., 2002. Organic carbon in shelf seas: sinks or sources, processes and products. Continental Shelf Research 22, 691–717.

Deuser, W.G., 1973. Cariaco Trench: oxidation of organic matter and residence time of anoxic water. Nature 242, 601–603.

Deuser, W.G., Muller-Karger, F.E., Hemleben, C., 1988. Temporal variations of particle fluxes in the deep subtropical and tropical North Atlantic: Eulerian versus Lagrangian effects. Journal of Geophysical Research 93 (C6), 6857–6862.

Deuser, W.G., Muller-Karger, F.E., Evans, R.H., Brown, O.B., Esaias, W.E., Feldman, G.C., 1990. Surface-ocean color and deep-ocean carbon flux: how close a connection? Deep-Sea Research 37 (8), 1331–1343.

Ding, K., Gordon, H.R., 1995. Analysis of the influence of O_2. A-band absorption on atmospheric correction of ocean-color imagery. Applied Optics 34, 2068–2080.

Enfield, D.B., Mayer, D.A., 1997. Tropical Atlantic sea surface variability and its relation to El Niño–Southern Oscillation. Journal of Geophysical Research 102, 929–945.

Eppley, R.W., 1972. Temperature and phytoplankton growth in the sea. Fishery Bulletin 70, 1063–1085.

Etcheber, H., Heussner, S., Weber, O., Dinet, A., Durrieu de Madron, X., Monaco, A., Buscail, R., Miquel, J.C., 1996. Organic carbon fluxes and sediment biogeochemistry on the French Mediterranean and Atlantic margins. In: Ittekkot, V., Shafer, P., Honjo, S., Depetris, P.J. (Eds.), Particle Flux in the Ocean. SCOPE 57. Wiley, New York, pp. 223–241 (Chapter 12).

Falkowski, P.G., 2002. The ocean's invisible forest—marine phytoplankton play a critical role in regulating the Earth's climate. Could they also be used to combat global warming? Scientific American 287 (2), 54–61.

Falkowski, P.G., Barber, R.T., Smetacek, V., 1998. Biogeochemical controls and feedbacks on ocean primary production. Science 281, 200–206.

Fargion, G., 1999. SIMBIOS: NRA contracts. SIMBIOS Project 1999 Annual Report. NASA/TM-1999-209486, pp. 7–11.

Fargion, G.S., Mueller, J., 2000. Ocean Optics Protocols For Satellite Ocean Color Sensor Validation, Revision 2'', NASA/TM-2000-209966.

Geider, R.J., Delucia, E.H., Falkowski, P.G., Finzi, A.C., Grime, J.P., Grace, J., Kana, T.M., La Roche, J., Long, S.P., Osborne, B.A., Platt, T., Prentice, I.C., Raven, J.A., Schlesinger, W.H., Smetacek, V., Stuart, V., Sathyendranath, S., Thomas, R.B., Vogelmann, T.C., Williams, P., Woodward, F.I., 2001. Primary productivity of planet earth: biological determinants and physical constraints in terrestrial and aquatic habitats. Global Change Biology 7 (8), 849–882.

Giannini, A., Kushnir, Y., Cane, M., 2000. Interannual variability of Caribbean rainfall, ENSO and the Atlantic Ocean. Journal of Climate 13, 297–311.

Giannini, A., Cane, M., Kushnir, Y., 2001. Interdecadal changes in the ENSO teleconnection to the Caribbean region and the North Atlantic Oscillation. Journal of Climate 14, 2867–2879.

Gong, G.-C., Shia, F.-K., Liu, K.-K., Wen, Y.-H., Liang, M.-H., 2000. Spatial and temporal variation of chlorophyll a, primary productivity and chemical oceanography in the southern East China Sea. Continental Shelf Research 20, 411–436.

Gordon, H.R., Wang, M., 1994. Retrieval of water-leaving radiance and aerosol optical thickness over the oceans with SeaWiFS: a preliminary algorithm. Applied Optics 33, 443–452.

Hastings, D., Emerson, S., 1988. Oxidation of manganese by spores of a marine Bacillus: kinetic and thermodynamic considerations. Geochimica et Cosmochimica Acta 50, 1819–1824.

Haug, G., Pedersen, T., Sigman, D., Calvert, S., Nielsen, B., Peterson, L., 1998. Glacial/interglacial; variations in production and nitrogen fixation in the Cariaco Basin during the last 580 kyr. Paleoceanography 13 (5), 427–432.

Hoerling, M., Hurrell, J., Xu, T., 2002. Tropical origins for recent North Atlantic climate change. Science 292, 90–92.

Hu, C., Carder, K.L., Muller-Karger, F.E., 2001. How precise are SeaWiFS ocean color estimates? Implications of digitization-noise errors. Remote Sensing of Environment 76 (2), 239–249.

Hu, C., Montgomery, E.T., Schmitt, R.W., Muller-Karger, F.E., 2004. The dispersal of the Amazon and Orinoco River water in the tropical Atlantic and Caribbean Sea: observation from space and S-PALACE floats. Deep-Sea Research II, this issue [doi: 10.1016/j.dsr2.2004.04.001].

Hughen, K.A., Overpeck., J.T., Peterson, L.C., Trumbore, S., 1996a. Rapid climate changes in the tropical Atlantic region during the last deglaciation. Nature 380, 51–54.

Hughen, K.A., Overpeck., J.T., Peterson, L.C., Anderson, R.F., 1996b. The nature of varved sedimentation in the Cariaco Basin, Venezuela, and its paleoclimatic significance. In: Palaeoclimatology and Palaeoceanography from Laminated Sediments. Geological Society Special Publication No. 116, pp. 171–183.

Hughen, K.A., Overpeck, J.T., Lehman, S.J., Kashgarian, M., Southon, J., Peterson, L.C., Alley, R., Sigman, D.M., 1998. Deglacial changes in ocean circulation from an extended radiocarbon calibration. Nature 391, 65–68.

Hughen, K., Southon, J., Lehman, S., Overpeck, J., 2000. Synchronous radiocarbon and climate shifts during the last deglaciation. Science 290, 1951–1954.

Lidz, L., Charm, W.B., Ball, M.M., Valdes, S., 1969. Marine basins off the coast of Venezuela. Bulletin of Marine Science 19 (1), 1–17.

Longhurst, A.R., 1991. Role of the marine biosphere in the global carbon cycle. Limnology and Oceanography 36 (8), 1507–1526.

McClain, E.P., Pichel, W.G., Walton, C.C., Ahmad, Z., Sutton, J., 1983. Multi-channel improvements to satellite-derived global sea-surface temperatures. Advances in Space Research 2 (6), 43–47.

McClain, C.R., Cleave, M.L., Feldman, G.C., Gregg, W.W., Hooker, S.B., Kuring, N., 1998. Science quality SeaWiFS data for global biosphere research. Sea Technology 39, 10–16.

Minnett, P.J., 1991. Consequences of sea surface temperature variability on the validation and applications of satellite measurements. Journal of Geophysical Research 96 (C10), 18475–18489.

Mueller, J.L., Austin, R.W., 1992. Ocean optics protocols for SeaWiFS validation. In: Hooker, S.B., Firestone, E.R. (Eds.), NASA Goddard Space Flight Center, NASA Technical Memorandum 104566, Greenbelt, MD, Vol. 5, 43pp.

Mueller, J.L., Austin, R.W., 1995. Ocean optics protocols for SeaWiFS validation. In: Hooker, S.B., Firestone, E.R. (Eds.), NASA Goddard Space Flight Center, NASA Technical Memorandum 104566, Greenbelt, MD, Vol. 25, 67pp (Revision 1).

Muller-Karger, F.E., Varela, R., 1990. Influjo del Rio Orinoco en el Mar Caribe: observaciones con el CZCS desde el espacio. Memoria, Sociedad de Ciencias Naturales La Salle, Caracas, Venezuela. Tomo L, numero 133–134 and 361–390.

Muller-Karger, F.E., McClain, C.R., Fisher, T.R., Esaias, W.E., Varela, R., 1989. Pigment distribution in the Caribbean Sea: observations from space. Progress in Oceanography 23, 23–69.

Muller-Karger, F., Varela, R., Thunell, R., Scranton, M., Bohrer, R., Taylor, G., Capelo, J., Astor, Y., Tappa, E., Ho, T.-Y., Iabichella, M., Walsh, J.J., Diaz, J.R., 2000. The CARIACO project: understanding the link between the ocean surface and the sinking flux of particulate carbon in the Cariaco Basin. EOS, AGU Transactions 81(45), 529, 534, 535.

Muller-Karger, F.E., Varela, R., Thunell, R., Scranton, M., Bohrer, R., Taylor, G., Capelo, J., Astor, Y., Tappa, E., Ho, T.-Y., Walsh, J.J., 2001. Annual cycle of primary production in the Cariaco Basin: response to upwelling and implications for vertical export. Journal of Geophysical Research 106 (C3), 4527–4542.

O'Reilly, J.E., Maritorena, S., O'Brien, M.C., Siegel, D.A., Toole, D., Mitchell, B.G., Kahru, M., Chavez, F.P., Strutton, P., Cota, G.F., Hooker, S.B., McClain, C.R., Carder, K.L., Muller-Karger, F.E., Harding, L., Magnuson, A., Phinney, D., Moore, G.F., Aiken, J., Arrigo, K.R., Letelier, R., Culver, M., 2000. Ocean color chlorophyll a algorithms for SeaWiFS, OC2, and OC4: Version 4. In: Hooker, S.B., Firestone, E.R. (Eds.), SeaWiFS Postlaunch Technical Report Series, NASA Technical Memorandum 2000-206892, Vol. 11. NASA Goddard Space Flight Center, Greenbelt, MD, 51pp.

Overpeck, J., Peterson, L., Kipp, N., Rind, D., 1989. Climate change in the circum-North Atlantic region during the last deglaciation. Nature 338, 553–557.

Peterson, L.C., Overpeck, J.T., Kipp, N.G., Imbrie, J., 1991. A high-resolution late quaternary upwelling record from the anoxic Cariaco Basin, Venezuela. Paleoceanography 6, 99–119.

Peterson, L., Haug, G., Hughen, C., Rohl, U., 2000. Rapid changes in the hydrologic cycle of the tropical Atlantic during the last glacial. Science 290, 1947–1951.

Pilskaln, C.H., Paduan, J.B., Chavez, F.P., Anderson, R.Y., Berelson, W.M., 1996. Carbon export and regeneration in the coastal upwelling system of Monterey Bay, central California. Journal of Marine Research 54, 1149–1178.

Pouliquen, S., Harscoat, M.V., Bentamy, A., 1996. WNF Products—User Manual. Reference No. C2-MUT-W-01-IF. IFREMER/CERSAT, France, 57pp.

Redfield, A.C., Ketchum, B.H., Richards, F.A., 1963. The influence of organisms in the composition of sea water. In: Hill, M.N. (Ed.), The Sea. Interscience, New York, pp. 26–77 (Chapter 2).

Richards, F.A., 1975. The Cariaco Basin (Trench). Oceanography and Marine Biology-An Annual Review 13, 11–67.

Scranton, M.I., Astor, Y., Bohrer, R., Ho, T.-Y., Muller-Karger, F.E., 2001a. Controls on temporal variability of the geochemistry of the deep Cariaco Basin. Deep-Sea Research I 48 (7), 1605–1625.

Scranton, M.I., Astor, Y., Bohrer, R., Ho, T.-Y., Muller-Karger, F.E., 2001b. The effect of subsurface water mass intrusions on the geochemistry of the Cariaco Basin. Deep-Sea Research I 48, 1605–1625.

Scranton, M.I., Novelli, P.C., Loud, P.C., 1984. The distribution and cycling of hydrogen gas in the waters of two anoxic marine environments. Limnology and Oceanography 29, 993–1003.

Siegel, D.A., Maritorena, S., Nelson, N.B., Hansell, D.A., Lorenzi-Kayser, M., 2002. Global distribution and dynamics of colored dissolved and detrital organic materials. Journal of Geophysical Research 107 (C12), 3228–3242.

Strong, A.E., McClain, E.P., 1984. Improved ocean surface temperatures from space, Comparisons with drifting buoys. Bulletin of the American Meteorological Society 65 (2), 138–142.

Taylor, G., Scranton, M., Iabichella, M., Ho, T., Thunell, R., Varela, R., Muller-Karger, F.E., 2001. Chemoautotrophy in the redox transition zone of the Cariaco Basin: a significant source of mid-water organic carbon production. Limnology and Oceanography 46 (1), 148–163.

Thunell, R., 1998. Particle fluxes in a coastal upwelling zone: sediment trap results from Santa Barbara Basin, California. Deep-Sea Research II 45, 1863–1884.

Thunell, R., Tappa., E., Varela, R., Llano, M., Astor, Y., Muller-Karger, F., Bohrer, R., 1999. Increased marine sediment suspension and fluxes following an earthquake. Nature 398, 233–236.

Thunell, R., Varela, R., Llano, M., Collister, J., Muller-Karger, F., Bohrer, R., 2000. Organic carbon flux in an anoxic water column: sediment trap results from the Cariaco Basin. Limnology and Oceanography 45, 300–308.

Walsh, J.J., 1991. Importance of continental margins in the marine biogeochemical cycling of carbon and nitrogen. Nature 350, 53–55.

Walton, C.C., 1988. Nonlinear multichannel algorithms for estimating sea surface temperature with AVHRR satellite data. Journal of Applied Meteorology 27, 115–127.

Ward, B.B., Kilpatrick, K.A., Novelli, P.C., Scranton, M.I., 1987. Methane oxidation and methane fluxes in the ocean surface layer and in deep anoxic waters. Nature 327, 226–229.

Werne, J.P., Hollander, D.J., Lyons, T.W., Peterson, L.C., 2000. Climate-induced variations in productivity and planktonic ecosystem structure from the Younger Dryas to Holocene in the Cariaco Basin, Venezuela. Paleoceanography 15, 19–29.

Zhang, J.-Z., Millero, F.J., 1993. The chemistry of the anoxic waters in the Cariaco Trench. Deep-Sea Research I 40, 1023–1041.